Degradation of Ethylene Thiourea (ETU) with Three Fenton Treatment Processes

David A. Saltmiras and Ann T. Lemley*

Field of Environmental Toxicology, TXA, MVR Hall, Cornell University, Ithaca, New York, 14853

Anodic Fenton treatment (AFT), an electrochemical, hydroxyl radical oxidation treatment system, was developed for the degradation of aqueous pesticides and other aqueous organic wastes. AFT of ethylene thiourea (ETU) was optimized and compared with electrochemical Fenton treatment (EFT) and classic Fenton treatment (CFT). ETU is a known carcinogen and is an impurity and degradation product of the widely used ethylenebisdithiocarbamate (EBDC) fungicide group. ETU was degraded effectively in all treatment methods, with CFT being the most rapid; however, significant differences in degradation product profiles were noted over the course of treatments. AFT displayed the most efficient degradation of primary degradation products of ETU.

Keywords: *Ethylene thiourea; ETU; Fenton; hydroxyl; oxidation; radical*

INTRODUCTION

The handling and disposal of pesticide rinse water is a significant waste management issue in the US (Felsot, 1996, 1998). Cleanup technologies that utilize the highly reactive hydroxyl radical produced via the Fenton reaction (eq 1) have been widely accepted for a number of decades (Hapeman and Torrents, 1998). Much interest in the organic compound degradative ability of hydroxyl radicals led to the development of a wide variety of radical oxidation processes (Carey, 1992; Hapeman and Torrents, 1998). Anodic Fenton treatment (AFT) is an electrochemical, radical oxidation process for the degradation of aqueous organic pesticide waste. It was developed to improve the performance of electrochemical Fenton treatment (EFT), an innovative application of the Fenton reaction:

$$Fe^{2+} + H_2O_2 \rightarrow Fe^{3+} + OH^- + HO^\bullet \qquad (1)$$

Classic Fenton treatment (CFT) uses ferrous salts such as $FeSO_4 \cdot H_2O$ to react with H_2O_2 and produce hydroxyl radicals by the Fenton reaction. This method was successful in degrading aqueous solutions of atrazine (Arnold et al., 1995) and chlorophenols (Tang and Huang, 1996; Barbeni et al., 1987). Research investigating photo-Fenton systems include the degradation of 2,4-D, 2,4,5-T, atrazine, trifluralin, picloram, baygon, and carbaryl (Sun and Pignatello, 1993), and xylidines (Nadtochenko and Kiwi, 1998). The efficiency of such photo-Fenton systems over a range of pH solutions was investigated by Zepp et al. (1992) using nitrobenzene and anisole as hydroxyl radical probes or hydroxyl trapping molecules. Variations of the CFT method have been applied to degrade and desorb compounds in soils and aquifer materials, such as chloroaliphatic compounds (Watts et al., 1999), sorbed and nonaqueous phase liquid hexadecane (Watts and Stanton, 1999), chlorobenzenes (Watts et al., 1997), chlorinated organics (Ravikumar and Gurol, 1994), and quinoline and nitrobenzene (Miller and Valentine, 1995). CFT has also been investigated as a treatment, in conjunction with bioremediation, of atrazine and other *s*-triazine pesticide waste (Arnold et al., 1996) and PCBs (Carberry and Yang, 1994).

Aqueous effluents produced under CFT are of low pH and require pH adjustment prior to disposal. The hygroscopic nature of ferrous salts increases the difficulty in handling and accurate delivery of Fe^{2+}, and because batch solutions of ferrous salt solutions readily oxidize to ferric (Fe^{3+}) solutions they cannot be stored longer than a few hours at room temperature. Electrochemical addition of ferrous ions provides a simple remedy to these obstacles by delivering the ferrous ions via sacrificial anodes (Pratap & Lemley, 1994, 1998; Roe & Lemley, 1996; McClung and Lemley, 1994). Other electrochemical adaptations of the Fenton reaction were investigated by Sudoh et al. (1986) to oxidize phenol and Tomat and Vecchi (1971) to oxidize benzene.

The disadvantages of using EFT include that (1) degradation of contaminants is slower than it is in Classic Fenton Treatment; (2) sorption to iron solids may remove some of the target compounds and degradation products from solution rather than fully degrading them; and (3) hydroxide ion production at the cathode, with production of a circumneutral pH effluent, inhibits optimal Fenton chemistry conditions of low pH.

To overcome these limitations of EFT, while retaining the advantages of Fenton chemistry and electrochemical iron delivery, the authors developed AFT, which uses two electrochemical half-cells connected via a salt bridge (Figure 1). The waste treatment occurs in the anode half-cell where ferrous ions are delivered via a sacrificial iron anode (eq 2). In this half-cell a low pH is generated which prevents the formation of iron solids. The cathode half-cell contains uncontaminated water which is reduced (eq 3) at the graphite electrode, producing a high pH.

$$Fe \rightarrow Fe^{2+} + 2e^- \qquad (2)$$

$$2H_2O + 2e^- \rightarrow H_{2(g)} + 2OH^- \qquad (3)$$

* To whom correspondence should be addressed. Phone: (607) 255-3151. Fax: (607) 255-1093. E-mail: atl2@cornell.edu.

10.1021/jf000084v CCC: $19.00
Published on Web 10/21/2000

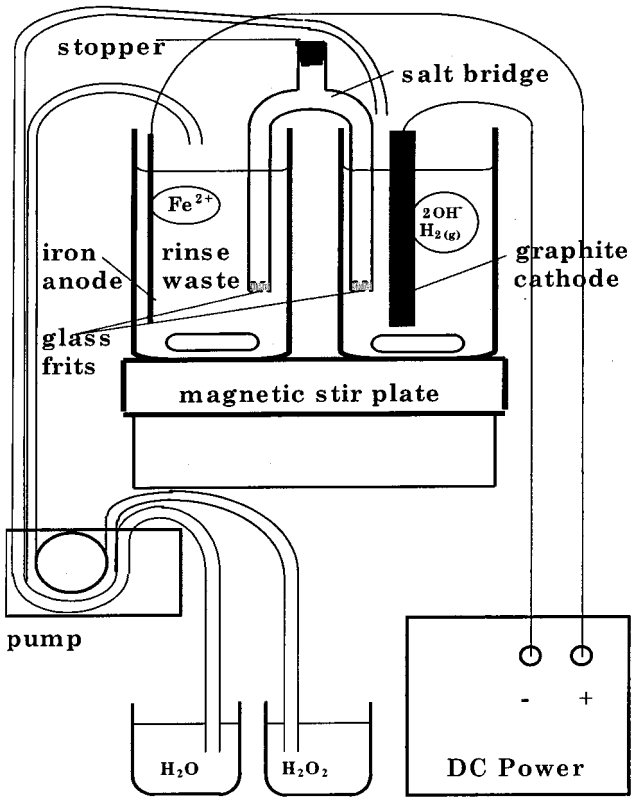

Figure 1. Anodic Fenton treatment apparatus.

Optimization of the AFT focused on the comparison of delivery ratios of Fe^{2+} to H_2O_2. This ratio for Fenton reagent delivery plays a critical role in the degradation efficiency of Fenton radical oxidation systems (Tang & Huang, 1996; Pratap & Lemley, 1998; Arnold et al., 1995), due to competing reactions shown in eqs 4−7 (Walling, 1975; Hill, 1992). Further competing reactions occur as hydroxyl radicals react with degradation products of the target compound.

$$H_2O_2 + HO^\bullet \rightarrow H_2O + HO_2^\bullet \quad (4)$$

$$Fe^{2+} + HO^\bullet \rightarrow Fe^{3+} + OH^- \quad (5)$$

$$H_2O_2 + Fe^{3+} \rightarrow Fe^{2+} + HO_2^\bullet + H^+ \quad (6)$$

$$Fe^{3+} + HO_2^\bullet \rightarrow Fe^{2+} + O_2 + H^+ \quad (7)$$

Combination of the AFT posttreatment half-cell solutions results in a circumneutral detoxified effluent containing iron solids. Consequently, iron solids may sorb the remaining unmineralized degradation products and heavy metals, such as zinc and manganese in fungicides such as Mancozeb. In AFT this process occurs after the Fenton treatment has completed maximum degradation in solution.

The same Fe^{2+}/H_2O_2 conditions for the optimal AFTs were applied to the comparison CFTs and EFTs. The ferrous ions and hydrogen peroxide delivery for all the CFTs were at the beginning of treatments, as done by Arnold et al. (1995), Haag and Yao (1992), Barbeni et al. (1987), and Dowling and Lemley (1995).

Ethylene thiourea (ETU) is characterized by low sorptivity to soils and is highly water soluble, and it is therefore a threat to groundwater quality (Fomsgaard, 1997). ETU is a degradation product, metabolite, and common impurity of up to 10% for the ethylenebisdithiocarbamate (EBDC) group of fungicides (Jacobsen and Bossi, 1997). EBDCs such as Mancozeb and Maneb are applied mostly to potatoes and tomatoes in the United States. Since 1977, toxicological assessment of EBDCs has been based on ETU (Vettorazzi et al., 1995). This compound led to the U.S. EPA proposed ban of EBDC fungicides in 1989 because of cancer risks, but the decision to ban was reversed in 1992. The Australian EPA (renamed Environment Australia) temporarily banned this class of fungicides until further evidence of an acceptable level of human health risk from ETU was established.

ETU toxicological investigations of interest focused on teratogenicity, mutagenicity, carcinogenicity, hepatoxicity, and thyroid function changes (Dearfield, 1994; Elia et al., 1995; Hurley et al., 1998; Nebbia and Fink-Gremmels, 1996; Pandey et al., 1990), and recently ETU was found to induce DNA damage to liver, kidney, lung, and spleen in mice (Sasaki et al., 1997).

Ethylene urea (EU) is a primary degradation product of ETU. Little toxicological data are available for EU other than it is not tumorigenic in rats fed at 0.1% EU for 150 days (Newsome, 1980). Very little attention has been given to the identification and quantification of such intermediates of pesticide degradation, such as ETU and EU, and their degradation pathways during chemical oxidations. Understanding the formation of intermediates, degradation pathways, and reactor optimization is critical prior to the use of AFT in the field (Chiron et al., 1997).

The goals of this research were to optimize the AFT of ETU on a benchtop scale and compare these results with the results of both CFT and EFT. Specific objectives were to (1) determine optimal Fe^{2+}/H_2O_2 delivery ratio for the AFT of ETU; (2) investigate effects of rate of delivery of Fenton reagents, Fe^{2+}, and H_2O_2, for the AFT of ETU at optimal Fe^{2+}/H_2O_2 delivery; and (3) compare the rate of formation and degradation of ETU primary transformation products for all treatment methods and propose degradation pathways of ETU for each treatment method.

MATERIALS AND METHODS

Chemicals. Chemicals obtained commercially were used as purchased, with the exception of hydrogen peroxide, which was diluted for AFT and EFT. Chemicals and suppliers were ETU (donated by Rhom and Haas); EU, 98% pure (Sigma Aldrich); $FeSO_4 \cdot H_2O$ (Fisher Scientific); HPLC grade methanol (Mallinckrodt); $KMnO_4$ (Fisher Scientific); 1−10 phenenthroline (in Hach Ferrover powder satchels); H_2O_2 (Mallinckrodt); and biodegradable scintillation counting liquid, BSC (Amersham).

Protocol Common to all Treatments. All treatments were for 100-mL batches of 200 μM ETU in a tall 200-mL beaker. The delivery ratio of Fe^{2+}/H_2O_2 was 1:10, determined in this work as optimal for AFT. This ratio was subsequently applied to the comparative CFTs and EFTs. Aliquots of 1.0 mL were removed from the treatment vessels over 10 min and hydroxyl radical activity was quenched by 50 μL of HPLC-grade methanol.

CFT Protocol. Ferrous sulfate heptahydrate, $FeSO_4 \cdot 7H_2O$ (103.3 mg), was added to the ETU solution, providing 3.7 mM Fe^{2+}. Treatment timing began on addition of 3.7 mmol of H_2O_2 of the approximate 30% hydrogen peroxide solution (about 375 μL, depending on the $KMnO_4$ titration), providing 37 mM H_2O_2 for a ratio of 1:10 of Fe^{2+}/H_2O_2, the same ratio as in the optimal AFTs. This ratio is close to the optimal Fe^{2+}/H_2O_2 of 1:11 for the CFT of any substrate as predicted in the model developed by Tang and Huang (1996). This method of batch treatment

with additions of the total amount of Fenton's reagent (ferrous ions and hydrogen peroxide) added at the beginning of treatments is consistent with previous CFT studies (Arnold et al., 1995; Dowling and Lemley, 1995; Barbeni et al., 1987).

AFT Protocol. ETU solutions were treated in the anode half-cell. The cathode half-cell contained 100 mL of nontreatment deionized water. Some salt bridge solution of saturated NaCl was added to each half-cell to provide sufficient initial conductivity for constant iron delivery throughout the treatments (1.0 mL to the anode, 4.0 mL to the cathode). Ferrous ion delivery from a single steel sacrificial anode (100 mm × 22 mm × 2 mm) at optimal treatments was achieved with a current of 0.12 amperes (2.08 mg/min Fe^{2+}). Hydrogen peroxide solution was added via a peristaltic pump at a rate of 0.5 mL/min, with an appropriate dilution of 30% hydrogen peroxide for the desired mole delivery ratio of Fe^{2+}/H_2O_2 of 1:10.

EFT Protocol. The EFT electrodes (anode and cathode) were three parallel steel plates (each 100 mm × 22 mm × 2 mm). Ferrous ion delivery from the sacrificial anode surfaces was set with a current of 0.06 amperes (same Fe^{2+} delivery as at 0.12 amperes with the single anode in AFT, 2.08 mg/min Fe^{2+}). Sodium chloride (0.02 g making 0.34 mM NaCl solution) was added as an electrolyte. Hydrogen peroxide solution was added in the same manner as in the AFT method. Samples were filtered through 0.2-mm polypropylene-encased nylon syringe filters (Alltech).

Ferrous Ion Delivery. Ferrous ion (Fe^{2+}) delivery was quantified for quality control by iron complexation with 1,10-phenanthroline (as Hach Ferrover powder) followed by UV−visible spectrophotometry (Perkin-Elmer λ-2) calibrated at 510 nm.

Hydrogen Peroxide Quantification. Hydrogen peroxide is prone to spontaneous degradation over time. Therefore, precise concentrations of the refrigerated 30% H_2O_2 stock were determined prior to treatments. Ten-fold dilutions of the stock H_2O_2 were titrated directly with acidified 0.1M $KMnO_4$, as in eq 8.

$$2\ KMnO_4 + 4\ H_2SO_4 + 5\ H_2O_2 \rightarrow 5\ O_2 + 2\ MnSO_4 + 2\ KHSO_4 + 8\ H_2O \quad (8)$$

Sample Analysis. The following HPLC method for ETU was developed for aqueous mobile-phase pH values of 3.0, to avoid column blockage from iron solid formation during analysis. Analyses were conducted on a Hewlett-Packard 1090 LC with diode array detector (DAD).

The Prism RP (Keystone Scientific Inc.) HPLC column parameters were 250 × 4.6 mm, 5 μm particles, 100 Å pore size. The mobile phase was isocratic, 95% water (pH adjusted to 3.0 with HCl, toward the low end of each column's pH limits of 2.5), 5% methanol with a 1.0 mL/min flow rate, constant temperature of 40 °C, and injection size of 50 μL. The DAD was set for chromatograms at 235 nm and 195 nm absorbance with retention time for ETU of 4.5 min at 235 nm absorbance; EU, 3.9 min at 195 nm absorbance; and Im-SO_3H, 3.2 min at 235 nm absorbance.

Standards for ETU and EU were used to compare HPLC retention times and UV spectra with limits of detection set at the lowest dilutions in the calibration curves, 1.4 μM and 1.0 μM, respectively. Calibration curves from ETU and EU standards had correlation values of $R^2 = 1.00000$ and $R^2 = 0.99999$ for the four serial dilutions of stock solutions.

Direct infusion MS of HPLC fractions of the 3.2 min HPLC peak for $ImSO_3H$ confirmation was conducted on a Bruker Esquire MS. The expected mass/charge ratio, (m+1)/z, for protonated $ImSO_3H$ is 151.

Mineralization of ^{14}C-Labeled ETU. ^{14}C-labeled ETU solutions were subjected to all three treatment processes in specially designed airtight Pyrex treatment vessels with horseshoe clamps. The CO_2 trap consisted of a 30-mL gas sparge tube with 20 mL of 1M 2-aminoethanol. Following treatments, the treatment solutions were sparged with 1.2 L of He gas over 3 h to eliminate dissolved CO_2. Blank experiments to quantify the $^{14}CO_2$ trapping efficiency were conducted by acidifying $NaH^{14}CO_3$.

Quantification of ^{14}C was conducted using a Beckman LS 7000 liquid scintillation counter. Samples were left in the dark overnight prior to analysis to avoid chemiluminescent counting errors.

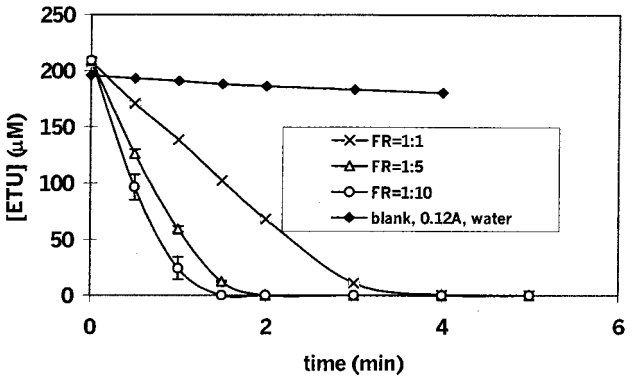

Figure 2. Anodic Fenton treatments of 200 μM ETU with different Fe^{2+}/H_2O_2 ratios, I = 0.12 amperes. FR refers to Fenton reagent or Fe^{2+}/H_2O_2 ratio.

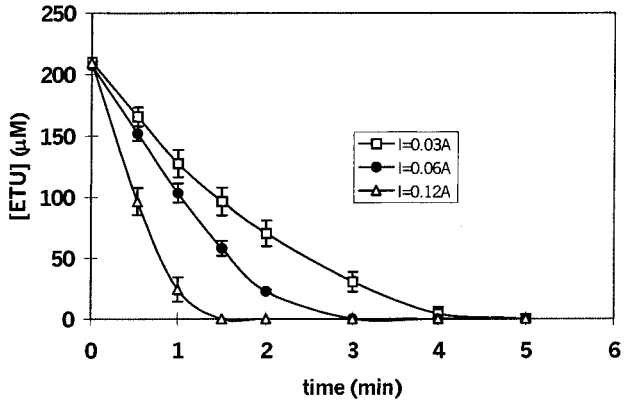

Figure 3. Anodic Fenton treatments of 200 μM ETU for Fe^{2+}/H_2O_2 = 1:10 with different addition rates. Error bars are the standard deviation of the mean for three separate treatments.

RESULTS AND DISCUSSION

The optimal ratio of Fe^{2+}/H_2O_2 additions for the AFT of ETU is shown in Figure 2 to be 1:10. Increased ratios of 1:20 were not found to improve the treatment efficiency (data not shown). Because hydrogen peroxide is able to quench hydroxyl activity (eq 4) (Pratap, 1996; Roe and Lemley, 1997; Pratap and Lemley, 1998; Walling, 1975; Haag and Yao, 1992) higher delivery rates of hydrogen peroxide were not considered.

The maximum current obtainable with the benchtop AFT equipment is 0.12 amperes, delivering ferrous ions at a rate of 37 μmol/minute (2.08 mg/minute). Figure 3 shows that this current appears to be a significant factor in improving degradation rate, but there is a practical limit to maximizing iron delivery electrochemically. Higher wattage transformers may provide sufficient voltage to generate greater currents, but these present safety issues in the laboratory. Therefore, AFT experiments were conducted at 0.12 amperes.

The degradation of ETU during AFT and EFT fit a zero-order rate. Regression equations below describe the degradation data shown in Figure 4 for AFT (eq 9) and EFT (eq 10), where C = concentration of ETU and t = time in minutes. AFT and EFT were equally efficient in the degradation of ethylene thiourea. This was

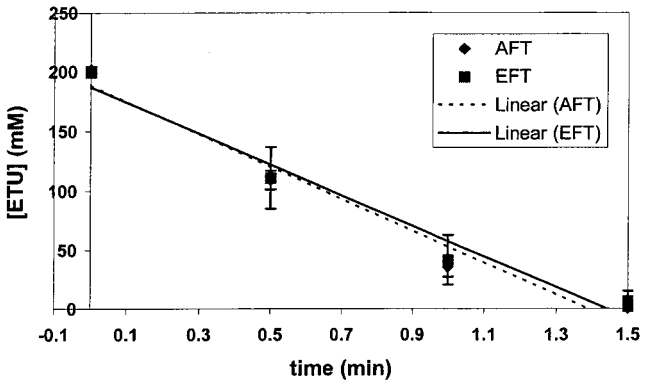

Figure 4. Comparison of anodic and electrochemical Fenton treatments in the degradation of 200 μM ETU, Fe^{2+}/H_2O_2 = 1:10. Error bars are the standard deviation of the mean for three separate treatments.

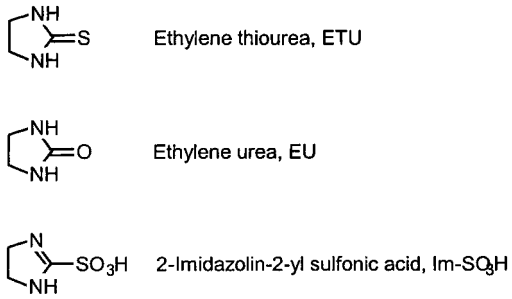

Figure 5. Chemical structures of ethylene thiourea (ETU), ethylene urea (EU), and 2-imidazolin-2-yl sulfonic acid (Im−SO_3H).

expected because EFT proved to be highly efficient in the degradation of water soluble pesticides such as metolachlor (Pratap and Lemley, 1998) and malathion (Roe and Lemley, 1996). Hydroxyl radical reactions with organic compounds are typically second or pseudo-first order. However, the limiting step in AFT degradation appears to be the hydroxyl radical generation, controlled by the Fe^{2+} and hydrogen peroxide delivery for the Fenton reaction. The maximum current for the system of 0.12 amperes delivers ferrous ions at 37 μmol/minute, which is therefore the maximum hydroxyl radical rate of production. As ETU degrades, the concentration of degradation products, which compete for hydroxyl radicals, increases. The kinetics of ETU degradation during AFT is therefore restricted by both the rate of hydroxyl radical generation and the increasing competition for hydroxyl radicals.

$$C = 188.5 - 135.7 \times t, \text{ where } R^2 = 0.965 \quad (9)$$

$$C = 187.0 - 129.7 \times t, \text{ where } R^2 = 0.967 \quad (10)$$

CFT is more rapid than both the AFT and EFT in the degradation of ethylene thiourea, fully degrading a 200 μM solution of ETU in less than 30 s (data not shown).

Two proposed degradation products, ethylene urea (EU) and the sulfonic acid of ETU, 2-imidazolin-2-yl sulfonic acid (Im-SO_3H), (chemical structures shown in Figure 5), were detected in all treatments of ETU.

Because no commercial standard was available for Im-SO_3H, it was synthesized in the laboratory as a minor product of 2-imidazoline synthesis (eq 11) as described by James et al. (1995). This synthesis involves a temperature-controlled reaction between ETU and hydrogen peroxide, producing 2-imidazoline (2-Im), EU, and Im-SO_3H. The chromatogram of the synthesis solution had four main peaks, two of which matched the standards of ETU and EU. Direct-infusion MS of the fraction corresponding to the HPLC peak at 3.2 min contained an ion at *m/z* 151, the expected value for the protonated ion for Im-SO_3H. The detection of Im-SO_3H, however, is considered to be tentative, as full confirmation employing MS/MS was not possible in this investigation. The fourth HPLC peak in the synthesis reaction, assumed to be 2-imidazoline, could not be found in the ETU treatment samples. Quantitative HPLC calibration could not be undertaken for Im-SO_3H, as no standard was available.

$$\text{ETU} + H_2O_2 \rightarrow \text{2-Im (major product)} + \text{EU} + \text{Im-}SO_3H \quad (11)$$

Significant differences in the rates of production and subsequent degradation of the two primary degradation products, EU and Im-SO_3H, were seen for the three treatment types. Chromatograms for the stock ETU solution (Figure 6) and 1.5 min into each treatment (Figures 7−9 for AFT, EFT, and CFT, respectively) show rapid ETU degradation and different amounts of degradation products. The EU concentration profile (Figure 10) shows that AFT produced very small quantities of EU, which were rapidly degraded. EFT produced significantly higher concentrations of EU than the other two treatments and did not fully degrade this primary degradation product within 10 min of treatments. CFT produced EU rapidly in the first 30 s, followed by a slow and steady increase in concentration.

The Im-SO_3H concentration profile also varied with each treatment (Figure 11). Although AFT produced the highest concentrations, degradation was complete within the 10 min treatments. EFT did not fully degrade the Im-SO_3H. CFT displayed a rapid production of Im-SO_3H, which was slowly decreased in concentration over the treatment, leaving the highest concentration of the three treatments after a 10-min period.

The degradation product profiles for AFT and EFT of ETU in Figures 10 and 11 are the typical bell-shaped curves described by Chiron et al. (1997), confirming that EU and ImSO_3H did undergo further degradation.

The degradation product profiles during CFT suggest rapid initial degradation of ETU and its degradation products, followed by very slow degradation of the degradation products. Figures 10 and 11 show that CFT degradation product profiles are not bell-shaped, and therefore the EU and ImSO_3H which formed after the initial rapid hydroxyl radical generation of the first 30 s did not undergo significant subsequent degradation during CFT.

Analysis of Figures 10 and 11 provides insight into the degradation pathways for ETU in each of the treatment methods, and these are summarized in Figure 12. AFT primarily produces Im-SO_3H and a small quantity of EU, both of which are subsequently degraded. EFT results in the production of both Im-SO_3H and EU, neither of which is fully degraded in the time period investigated. CFT shows a preferential pathway of ETU to Im-SO_3H to EU, as increases in EU concentration over time qualitatively correlate with Im-SO_3H concentration decreases over time. However, the rapid concentration increases in both EU and Im-SO_3H during the first 30 s of CFT suggests both degradation products form readily.

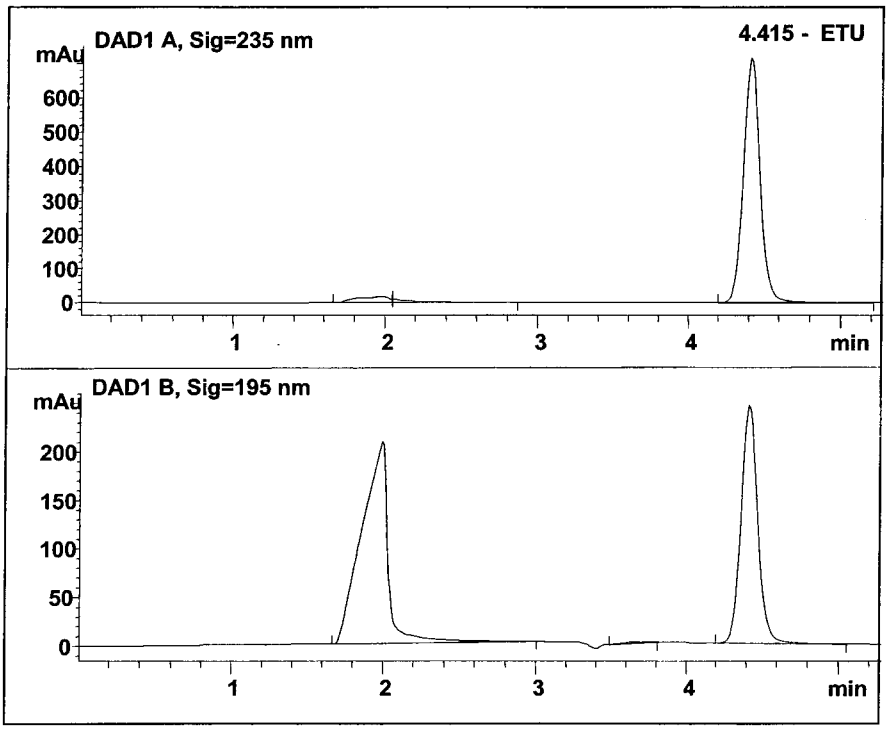

Figure 6. Chromatograms of 200 μM ETU stock at $t = 0$. Sloping peak at 1.7−2.1 min in the 195 nm chromatogram is due to sodium chloride electrolyte.

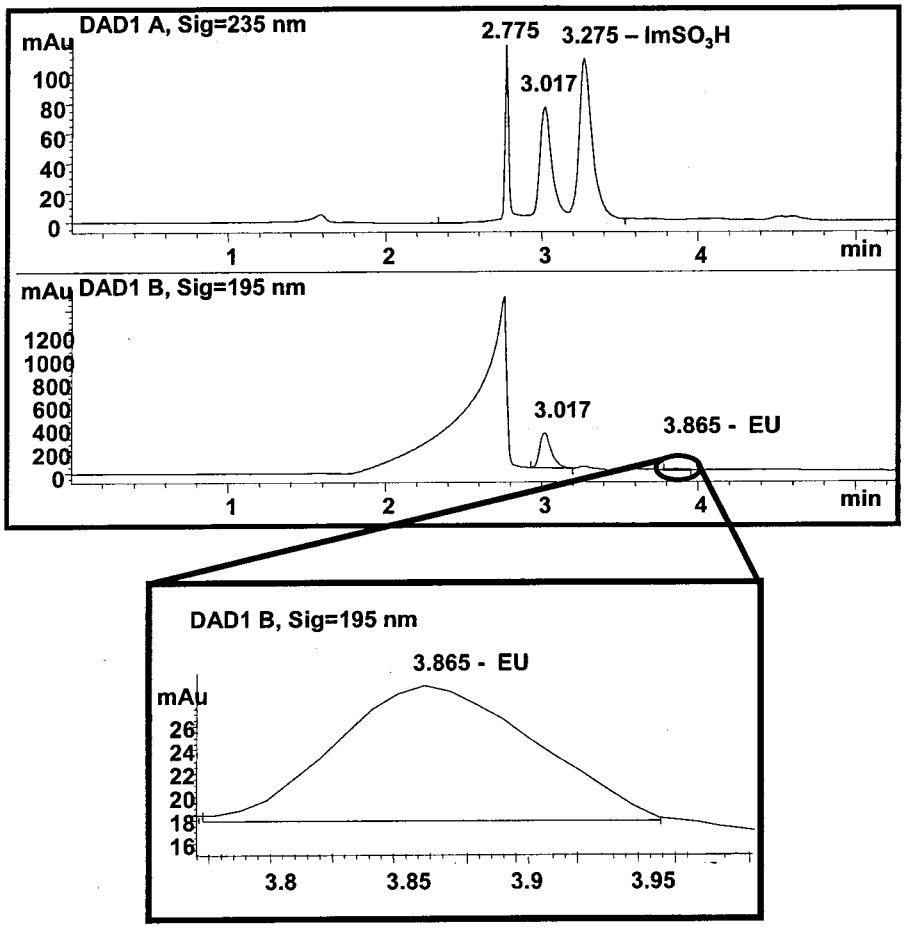

Figure 7. Chromatograms of AFT of 200 μM ETU at $t = 1.5$ min treatment. No ETU detected, [EU] = 10 μM.

^{14}C data for AFT and EFT could not be used to quantify the extent of mineralization during treatments. A full mass balance for ^{14}C was obtained for the CFT, but the AFT and EFT had less than 60% ^{14}C recovery. Repeated attempts at obtaining full ^{14}C mass balances for AFT and EFT only replicated the ^{14}C loss, suggesting

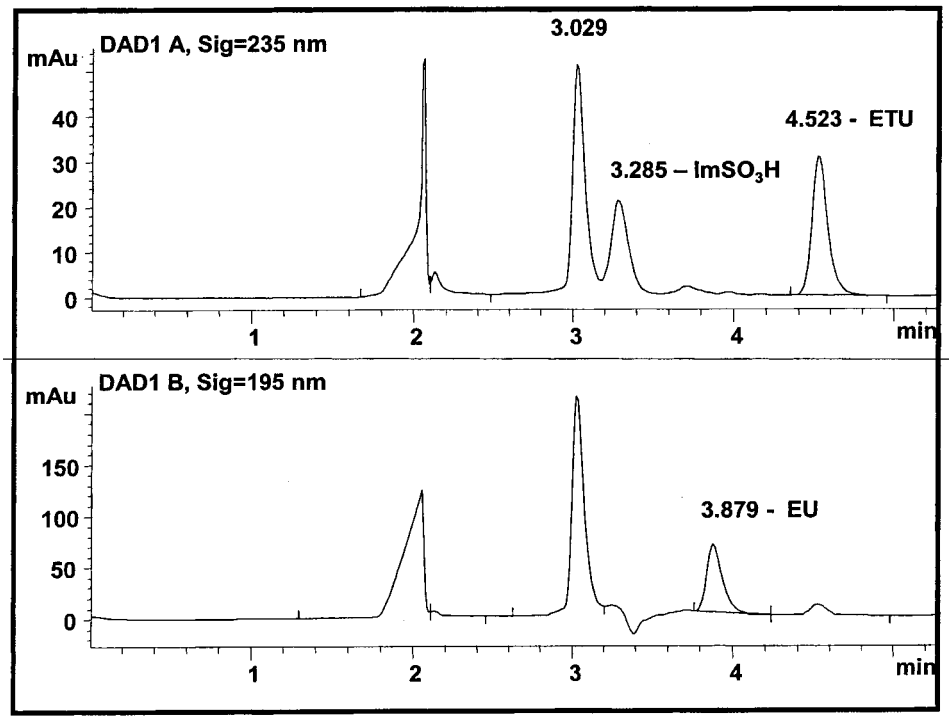

Figure 8. Chromatograms of EFT of 200 μM ETU at t = 1.5 min treatment. [ETU] = 10 μM, [EU] = 80 μM.

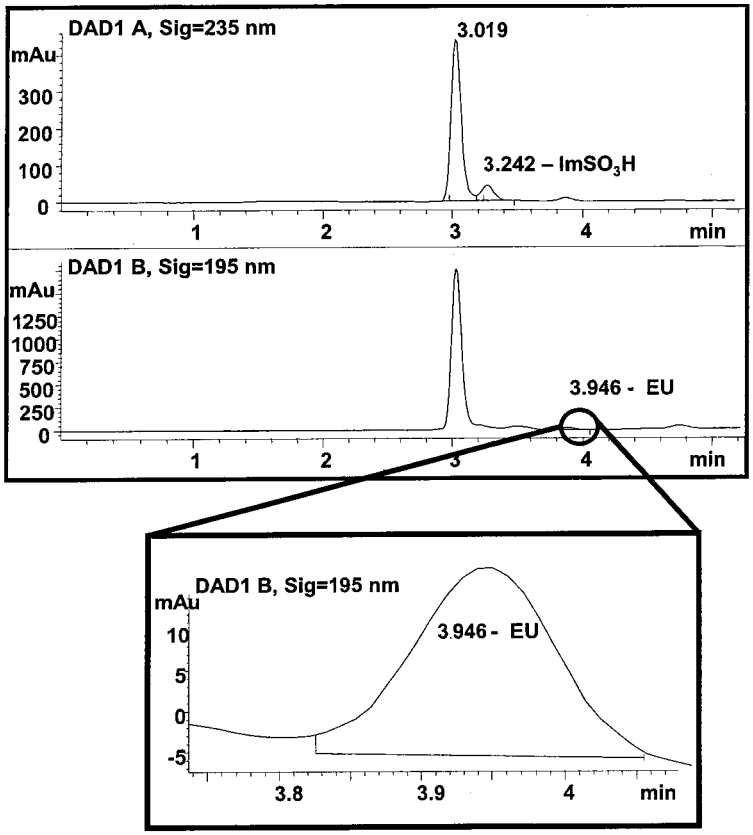

Figure 9. Chromatograms of CFT of 200 μM ETU at t = 1.5 min treatment. No ETU detected, [EU] = 21 μM.

^{14}C sorption somewhere in the airtight apparatus. Full ^{14}C recovery has been obtained for the AFT investigations of atrazine degradation, confirming the integrity of the ^{14}C apparatus for AFT. The lack of a mass balance in this work is an actual result, perhaps due to volatile intermediates that do not trap like CO_2. All treatments had some $^{14}CO_2$ detected in the CO_2 trap (Table 1). The trapping efficiency for CO_2 was determined to be 82% from the $NaH_{14}CO_3$ acidification and purging experiments.

The Fenton reactants were delivered at the beginning of each CFT, as is consistent with other investigations reported in the literature (Arnold et al., 1995; Dowling and Lemley, 1995; Barbeni et al., 1987). However,

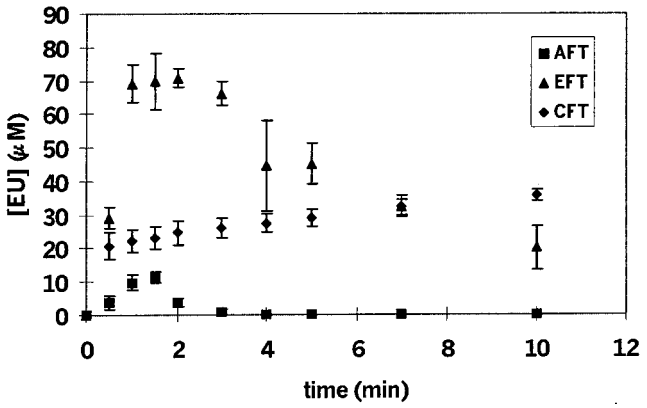

Figure 10. Concentration profile for ethylene urea (EU) during anodic, electrochemical, and classic Fenton treatments of 200 μM ETU, Fe^{2+}/H_2O_2 = 1:10. Error bars are the standard deviation of the mean for three separate treatments.

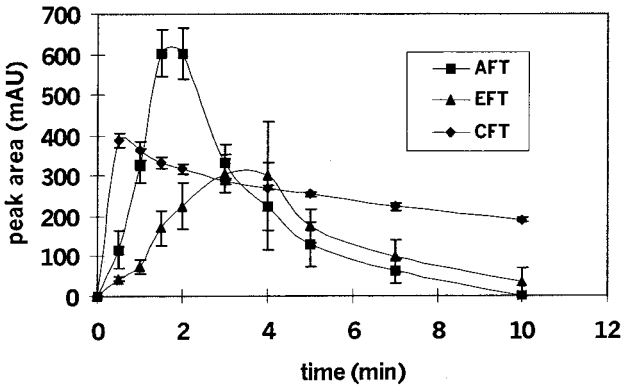

Figure 11. Concentration profile for Im−SO_3H during anodic, electrochemica,l and classic Fenton treatments of 200 μM ETU, Fe^{2+}/H_2O_2 = 1:10. Error bars are the standard deviation of the mean for three separate treatments.

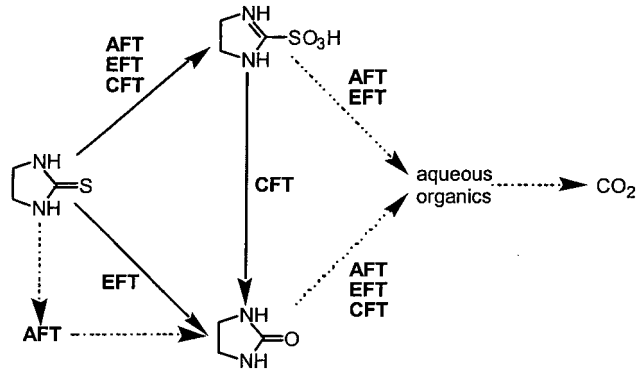

Figure 12. Primary degradation pathways for ETU under anodic, electrochemical, and classic Fenton treatments. Bold arrows are major pathways; dashed arrows are minor pathways.

during AFT and EFT the same quantity of Fenton reactants as in CFT were delivered at a uniform rate over the 10 min treatments and at constant Fe^{2+}/H_2O_2 ratios. Therefore, the AFT and EFT have sustained hydroxyl radical production throughout the experiments, allowing for continual degradation of ETU and its degradation products. CFT, however, does not sustain hydroxyl radical production throughout the experiments, therefore limiting degradation of EU and Im-SO_3H.

Although CFT is rapid, hydroxyl radical generation is short-lived, which limits the extent of degradation

Table 1. Results of ^{14}C-Labeled ETU Mineralization Investigations[a]

treatment	^{14}C recovery (%)	std dev of ^{14}C recovery (%)	mineralization to CO_2 (%)	std dev of mineralization to $^{14}CO_2$ (%)
CFT	98.8	9.2	21.0	3.2
AFT	56.2	8.9	4.4	0.6
EFT	54.1	18.9	9.3	7.8

[a] Standard deviations are from three separate treatments for each treatment method.

along the pathways to other intermediate compounds and mineralization, following the initial rapid production of hydroxyl radicals. It is expected that degradation pathways are via aqueous organic intermediates prior to mineralization to CO_2, as summarized in Figure 12. According to Watts and Stanton (1999), such intermediates may not be mineralized by hydroxyl radicals, but rather by other transient oxygen species, which can result from residual hydrogen peroxide. This conclusion is based on work done by Dorfman and Adams (1973), who compiled data on hydroxyl radical activity in aqueous solutions. Dorfman and Adams (1973) suggest that hydroxyl radical reactivity toward esters and carboxylic acids is generally slower than those for alcohols. However, all the rate constants are still extremely high, on the order of 10^7-10^{10} $M^{-1}s^{-1}$, approaching diffusion rates. Thus, in the work reported, because hydroxyl radicals are being produced continuously during treatment it is reasonable to propose that they degrade intermediates.

Steiner and Babbs (1990) adapted CFT in order to quantify hydroxyl radical production. They did this by gradual addition of hydrogen peroxide to a solution containing the desired amount of ferrous (Fe^{2+}) ions. This approach, however, starts with a very high Fe^{2+}/H_2O_2 ratio, because all Fe^{2+} is initially in the reaction vessel, and is not optimal for hydroxyl radical production via the Fenton reaction because of the large initial excess ferrous ion concentration. Tang and Huang (1996) stress that neither ferrous ions nor hydrogen peroxide should be over-dosed for the maximal reaction rate to be achieved. As hydrogen peroxide is added, the Fenton reaction proceeds, along with other oxidative reactions, resulting in an unknown ferrous ion concentration and an unknown ratio of Fe^{2+}/H_2O_2. A more controlled approach to applying CFT and to maintaining sustained hydroxyl radical production as in the AFT, would be to slowly add ferrous salt solution and hydrogen peroxide solution separately to the treatment vessel. However, the AFT method developed in this paper is, in essence, an attempt to optimize the CFT, without the drawbacks of unstable solutions of ferrous ion made from hygroscopic salts that are difficult to handle and by providing a simple way to produce an effluent with circumneutral pH. It is thus important to compare the AFT studies with CFT studies similar to those reported in the literature, as per the methods described herein.

AFT effluent contains high concentrations of chloride ions from the salt bridge electrolyte, on the order of 0.2 M. Concentrations of chloride above the millimolar level at pH 3 (the pH of the AFT effluent from the anode treatment half-cell) have been reported to inhibit hydroxyl radical attack via scavenging (Pignatello, 1992; Tang and Huang, 1996). Therefore, the authors believe that alternative half-cell separation techniques such as

membranes, may prove the AFT even more efficient in degrading ETU than is currently recognized.

The power supply used in both AFTs and EFTs was a variable-voltage DC power supply with a maximum voltage of 30 V. The maximum possible power supplied for the 10 min treatments for AFT (0.12 amperes) and EFT (0.06 amperes) are 6.0×10^{-4} kWh and 3.0×10^{-4} kWh, respectively. However, during treatments, voltages varied from less than 10 V to nearly 30 V, making actual power used significantly less. The New York State Electric and Gas (NYSEG) residential charge for electricity is 12.9 cents per kWh, costing AFT, at most, 0.0077 cents for electricity per treatment (77 cents/1000 Ls). The maximum electricity cost for EFT would be 0.0038 cents per treatment (38 cents/1000 Ls). Final cost estimates must await scaling to a full flow-through system, as major apparatus redesign will be necessary.

A half-life of 2.5 days was determined for ETU in agricultural soils in the Philippines − a tropical environment conducive to microbial activity (Jacobsen and Bossi, 1997). Much greater half-lives for ETU would be expected in soils of more temperate regions such as a those in the United States where EBDC fungicides are applied. ETU is a very stable compound in water with great potential for ground and surface water contamination. Therefore, a flow-through Anodic Fenton Treatment of EBDC fungicide wastewaters would provide a valuable means of on-site treatment and disposal of EBDC fungicide wastewaters to degrade ETU, EU, and Im-SO_3H. Such a system coupled with bioremediation embraces the view of Felsot (1996), that cleanup should integrate physical, chemical, and biological technologies.

CONCLUSIONS

Optimal treatment conditions for the anodic Fenton treatment of ETU with current-controlled ferrous ion delivery was found to be an Fe^{2+}/ H_2O_2 addition ratio of 1:10 delivered at the maximum delivery rate, as limited by current flow.

These conditions provided equivalent degradation efficiencies for ETU in both AFT and EFT. Although ETU was most rapidly degraded under classic Fenton treatment, primary degradation products were most effectively degraded under anodic Fenton treatment.

AFT holds promise as a new, practical radical oxidation process for on-site treatment and disposal of aqueous pesticide waste. Further research on flow-through designs, salt-bridge alternatives, and other significant pesticides of interest will be necessary before the practicality of the anodic Fenton treatment of aqueous pesticide waste can be determined.

ACKNOWLEDGMENT

Input from Song Hong, Department of Textiles and Apparel, Cornell University, was appreciated. Thanks to Andco Environmental Processes, Amherst, NY, for providing the DC power supply, electrodes, and open discussion. Technical support from Michael Ames of the College of Human Ecology, Cornell University, was invaluable.

LITERATURE CITED

Arnold, S. M.; Hickey, W. J.; Harris, R. F. Degradation of atrazine by Fenton's reagent: condition optimization and product quantification. *Environ. Sci. Technol.* **1995**, *29*, 2083−2089.

Arnold, S. M.; Hickey, W. J.; Harris, R. F.; Talaat, R. E. Integrating chemical and biological remediation of atrazine and *s*-triazine-containing pesticide wastes. *Environ. Toxicol. Chem.* **1996**, *15*(8), 1255−1262.

Barbeni, M.; Minero, C.; Pelizzetti, E. Chemical degradation of chlorophenols with Fenton's reagent. *Chemosphere* **1987**, *16*(10−12), 2225−2237.

Carberry, J. B.; Yang, S. Y. Enhancement of PCB congener biodegradation by pro-oxidation with Fenton's reagent. *Water Sci. Technol.* **1994**, *30*(7), 105−113.

Carey, J. H. An introduction to advanced oxidation processes (AOP) for destruction of organics in wastewater. *Water Poll. Res. J. Canada* **1992**, *27*(1), 1−21.

Chiron S.; Fernandez-Albam, A. R.; Rodriguez, A. Pesticide chemical oxidations processes: an analytical approach. *Trends Anal. Chem.* **1997**, *9*, 518−527.

Dearfield, K. L. Ethylene thiourea (ETU). A review of the genetic toxicity studies. *Mutat. Res.* **1994**, *317*, 111−132.

Dorfman, L. M.; Adams, G. E. *Reactivity of the Hydroxyl Radical in Aqueous Solutions*, Report No. NSRDS−NBS-46. National Bureau of Standards: Washington, DC, 1973; pp. 22−31.

Dowling, K. C.; Lemley, A. T. Organophosphate insecticide degradation by nonammended and cupric ion-ammended Fenton's reagent in aqueous solution. *J. Environ. Sci. Health, B* **1995**, *30*(5), 585−604.

Elia, M. C.; Arce, G.; Hurt, S. S.; O'Neill, P. J.; Scribner, H. E. The genetic toxicology of ethylenethiourea: a case study concerning the evaluation of a chemical's genotoxic potential. *Mutat. Res.* **1995**, *341*, 141−149.

Felsot, A. S. Options for cleanup and disposal of pesticide wastes generated on a small scale. *J. Environ. Sci. Health, B* **1996**, *31*(3), 365−381.

Felsot, A. S. User sites and the generation of pesticide waste. In *Pesticide Remediation in Soils and Water;* P. C. Kearney and T. Roberts, Eds.; Wiley: New York, 1998; Chapter 1, pp. 1−20.

Fomsgaard, I. S. Modelling the mineralization kinetics for low concentrations of pesticides in surface and subsurface soil. *Ecol. Modell.* **1997**, *102*, 175−208.

Haag, W. R.; Yao, C. C. Rate constants for reaction of hydroxyl radicals with several drinking water contaminants. *Environ. Sci. Technol.* **1992**, *25*, 1005−1013.

Hapeman, C. J.; Torrents, A. Direct Radical Oxidation Processes. In *Pesticide Remediation in Soils and Water;* P. C. Kearney and T. Roberts, Eds.; Wiley: New York, 1998; Chapter 8, pp. 161−180.

Hill, C. L. The use of polyoxometalates in reactions with hydrogen peroxide. In *Catalytic Oxidations with Hydrogen Peroxide as Oxidant*; Giorgio Strukul, Ed.; Kluwer Academic: Dordrecht, The Netherlands, 1992; Chapter 8, pp. 253−280.

Hurley, P. M.; Hill, R. N.; Whiting, R. J. Mode of carcinogenic action of pesticides inducing thyroid follicular cell tumors in rodents. *Environ. Health Perspect.* **1998**, *106*(8), 437−445.

Jacobsen, O. S.; Bossi, R. Degradation of ethylenethiourea (ETU) in oxic and anoxic sandy aquifers. *FEMS Microbiol. Rev.* **1997**, *20*, 539−544.

James, P. J.; Quistad, G. B.; Casida, J. E. Ethylenethiourea *s*-oxidation products: preparation, degradation, and reaction with proteins. *J. Agric. Food Chem.* **1995**, *43*, 2530−2535.

McClung, S. M.; Lemley, A. T. Electrochemical treatment and HPLC analysis of wastewater containing acid dyes. *Wastewater Treatment* **1994**, *26*(3), 17−22.

Miller, C. M.; Valentine, R. L. Oxidation behavior of aqueous contaminants in the presence of hydrogen peroxide and filter media. *J. Hazard. Mater.* **1995**, *41*, 105−116.

Nadtochenko, V.; Kiwi, J. Primary Photochemical Reactions in the Photo-Fentonsystem with ferric chloride. 1. A case study of xylidine oxidation as a model compound. *Environ. Sci. Technol.* **1998**, *32*, 3273−3281.

Nebbia, C.; Fink-Gremmels, J. Acute effects of low doses of zineb and ethylenethiourea on thyroid function in the male rat. *Bull. Environ. Contam. Toxicol.* **1996**, *56*, 847−852.

Newsome, W. H. Ethylenebisdithiocarbamates and their degradation products. In *Analytical Methods for Pesticides and Plant Growth Regulators, Vol. XI*; G. Zweig, J. Sherma, Eds.; Academic Press: New York, 1980; Chapter 9, 197−226.

Pandey, M.; Raizada, R. B.; Dikshith, T. S. S. 90-day oral toxicity of ziram: a thyrostatic and hepatotoxic study. *Environ. Pollut.* **1990**, *65*, 311−322.

Pratap, K.; Lemley, A. T. Fenton electrochemical treatment of aqueous atrazine and metolachlor. *J. Agric. Food Chem.* **1998**, *46*, 3285−3291.

Pratap, K. Fenton electrochemical treatment of Metolachlor and Atrazine. Ph.D. Dissertation, Cornell University, Ithaca, NY, May, 1996.

Pratap, K.; Lemley, A. T. Electrochemical peroxide treatment of aqueous herbicide solutions. *J. Agric. Food Chem.* **1994**, *42*, 209−215.

Pignatello, J. J. Dark and photoassisted Fe^{3+}-catalyzed degradation of chlorophenoxy herbicides by hydrogen peroxide. *Environ. Sci. Technol.* **1992**, *26*, 944−951.

Roe, B. A.; Lemley, A. T. Treatment of two insecticides in an electrochemical Fenton system. *J. Environ. Sci. Health, B* **1997**, *32*(2), 261−281.

Ravikumar, J. X.; Gurol, M. D. Chemical oxidation of chlorinated organics by hydrogen peroxide in the presence of sand. *Environ. Sci. Technol.* **1994**, *28*, 394−400.

Sasaki, Y. F.; Izumiyama, F.; Nishidate, E.; Matsusaka, N.; Tsuda, S. Detection of rodent liver carcinogen genotoxicity by the alkaline single-cell gel electrophoresis (Comet) assay in multiple mouse organs (liver, lung, spleen, kidney and bone marrow). *Mutat. Res.* **1997**, *391*, 201−214.

Steiner, M. G.; Babbs, C. F. Quantitation of the hydroxyl radical by reaction with dimethyl sulfoxide. *Arch. Biochem. Biophys.* **1990**, *278*(2), 478−481.

Sudoh, M.; Kodera, T.; Sakai, K.; Zhang, J. Q.; Koide, K. Oxidative degradation of aqueous phenol effluent with electrogenerated Fenton's reagent. *J. Chem. Eng. Jpn.* **1986**, *19*(6), 513−518.

Sun, Y.; Pignatello, J. J. Activation of peroxide by iron (III) chelates for abiotic degradation of herbicides and insecticides in water. *J. Agric. Food Chem.* **1993**, *41*, 308−312.

Tang, W. Z.; Huang, C. P. 2,4-dichlorophenol oxidation kinetics by Fenton reagent. *Environ. Technol.* **1996**, *17*, 1371−1378.

Tomat, R.; Vecchi, E. Electrocatalytic production of OH radicals and their oxidative addition to benzene. *J. Appl. Electrochem.* **1971**, *1*, 185−188.

Vettorazzi, G.; Waldermar, F. A.; Buron, G. J.; Jaeger, R. B.; Puga, F. R.; Rahde, A. F.; Reyes, F. G.; Schvartsman, S. International safety assessment of pesticides: dithiocarbamate pesticides, ETU and PTU − a review and update. *Teratog., Carcinog., Mutagen.* **1995**, *15*, 313−337.

Walling, C. Fenton's Reagent Revisited. *Acc. Chem. Res.* **1975**, *8*, 125−131.

Watts, R. J.; Bottenberg, B. C.; Hess, T. F.; Jensen, M. D.; Teel, A. L. Role of reductants in the enhanced desorption and transformation of chloroaliphatic compounds by modified Fenton's reactions. *Environ. Sci. Technol.* **1999**, *33*, 3432−3437

Watts, R. J.; Jones, A. P.; Chen, P.; Kenny, A. Mineral-catalyzed Fenton-like oxidation of sorbed chlorobenzenes. *Water Environ. Res.* **1997**, *69*(3), 269−275.

Watts, R. J.; Stanton P. C. Mineralization of sorbed and NAPL-phase hexadecane by catalyzed hydrogen peroxide. *Water Res.* **1999**, *33*(6), 1405−1414.

Zepp R. G.; Faust, B. C.; Hoigné, J. Hydroxyl radical formation in aqueous reactions (pH 3−8) of iron (II) with hydrogen peroxide: the photo-Fenton reaction. *Environ. Sci. Technol.* **1992**, *26*, 313−319.

Received for review January 19, 2000. Revised manuscript received September 7, 2000. Accepted September 11, 2000. Funding for this investigation was provided by the USDA (NRICGP # 9604166 and Hatch Regional Research) and the College of Human Ecology, Cornell University.

JF000084V